Energy distributions and effective temperatures in the packing of elastic sheets

Stephanie Deboeuf, Mohktar Adda-Bedia, Arezki Boudaoud

Energy distributions and effective temperatures in the packing of elastic sheets

S. Deboeuf, M. Adda-Bedia and A. Boudaoud
Laboratoire de Physique Statistique de l'Ecole Normale Supérieure, CNRS UMR 8550, 24 rue Lhomond, 75005 Paris, France

The packing of elastic sheets is investigated in a quasi two-dimensional experimental setup: a sheet is pulled through a rigid hole acting as a container, so that its configuration is mostly prescribed by the cross-section of the sheet in the plane of the hole. The geometrical properties and energies of the branches forming the cross-section are broadly distributed. The distributions of energy have exponential tails yielding effective temperatures. Two sub-systems can be defined: in contact with the container and within the bulk. While the geometrical properties differ between the sub-systems, their energy distributions are identical, indicating that 'thermal equilibration' occurs.

PACS numbers: 64.70.qd 46.65.+g 68.55.-a, 46.32.+x,

The challenges raised by out-of-equilibrium systems are exemplified by granular materials [1] and glasses [2, 3], featuring complex energy landscapes and aging. Energy flow and thermal equilibration in such systems can be characterised by various effective temperatures [4, 5, 6]; however, previous experimental studies [7, 8, 9, 10, 11, 12] only measured a temperature based on the ratio between fluctuations and response of the system. Here we present experiments on an singular and macroscopic out-of-equilibrium system, namely the packing of elastic sheets into quasi two-dimensional containers [13] and focus on the statistical properties of the configurations. We show that thermal equilibration occurs within the system although its geometrical properties are not uniform, enabling the definition of effective temperatures from the distributions of energy. Thus we obtain a macroscopic experimental system that could be used to test out-of-equilibrium statistical physics. Our results bear on the packing of flexible structures such as elastic rods [14, 15, 16], crumpled paper [17, 18, 19, 20], folded leaves in buds [21], chromatin in cell nuclei [22] or DNA in viral capsids [15, 23].

At equilibrium, systems with a large number of degrees of freedom are characterised by a single temperature T. On the one hand, the energy of one degree of freedom follows Boltzmann's distribution, the mean energy being proportional to T. On the other hand, T might be measured using the fluctuation-dissipation theorem (FDT), relating fluctuations of an observable to its response to an external field. Two main effective temperatures were introduced for systems out of equilibrium. The approach of Edwards [4] amounts to the replacement of T by an effective temperature in the distribution of energies; it can be extended to intensive thermodynamic parameters associated with global conserved quantities [6, 24, 25, 26]. The generalisation of the FDT [5] gives another effective temperature, which can be measured [7, 8, 9, 10, 11, 12, 27]. In many models, Edwards' and FDT temperatures are equal [28, 29, 30, 31] or proportional [32]. An experimental measurement of Edwards' temperature seems to be lacking as it is difficult to obtain energy distributions. Here we make this possible by investigating the packing of elastic sheets.

Fig. 1**a** represents the experimental set-up [13], inspired by the study of single d-cones [33]. We use circular polyester (polyethylene terephtalate) sheets of Young's modulus measured as $E = 5$ GPa, density 1.4 g/cm^3, various radii $r \sim 30$ cm and thicknesses $h \sim 0.1$ mm. At each realisation, a sheet is pulled from its center through a circular rigid hole of radius $R \sim 2$ cm. The values of the parameters (r, h, R) for each set of experiments are given in Table I. The hole is machined through a Plexiglas plate and its edges are rounded to form a toroidal convex shape, to avoid damaging the sheet. The center of

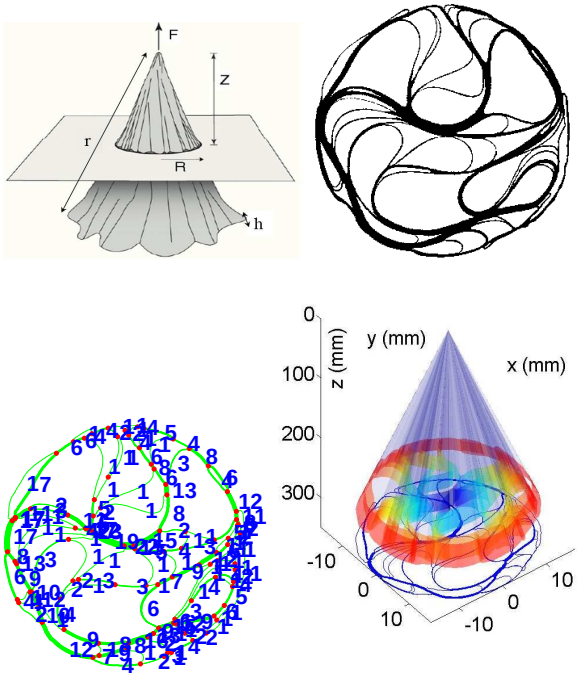

FIG. 1: The experiment. **a** Schematic of the set-up showing the radius of the sheet r, its thickness h, the radius of the hole R and the control parameter Z; the force F is measured with a dynamometer. **b** Thresholded picture of a horizontal cross-section from set i of experiments. **c** Analysed cross-section, showing the existence of multi-branches stacks delimited by two junction points. The number of branches is indicated near each stack. **d** 3D reconstruction assuming exact self-similarity of shape.

set	$h(\mu\text{m})$	$r(\text{cm})$	$B(\text{J})$	$R(\text{mm})$	$Z_\text{m}(\text{cm})$	p	$\#\mathcal{R}$
i	50	33	$7\,10^{-5}$	16.5	30	11%	33
ii	50	33	$7\,10^{-5}$	22.5	30	6%	16
iii	125	22	$1\,10^{-3}$	27	19	7%	16

TABLE I: Material parameters for the sheets used in experiments: thickness h, radius r and bending stiffness B; control parameters: hole radius R, maximal pulling distance Z_m, and packing ratio $p = 2hZ_\text{m}/R^2$; number of realisations $\#\mathcal{R}$.

the sheet is pierced and fixed to a dynamometer by means of a threaded mount of radius $R_c = 0.8$ cm. The sheet is pulled at a velocity of 0.5 mm/s, so that the distance Z, between the pulling point and the plane of the hole is our main control parameter. The measurement of the pulling force F during the compaction directly yields the work injected in the system $W = \int_0^Z F\text{d}z$.

The sheet might undergo two modes of deformation: bending and stretching. As bending is favoured energetically, a self-similar conical shape is expected [34], so that one cross-section approximately prescribes the whole shape of the sheet. A virtual cut across the sheet in the plane of the hole yields a one-dimensional rod of length $2\pi Z$, that grows within a disk of radius R as Z is increased. The experiment allows *isotropic* confinement to packing ratios p as high as 11%, where $p = 2Zh/R^2$ is the ratio of cross-sectional area of the sheet $2\pi Zh$ to the area of the hole πR^2.

In principle, configurations can be visualised from below. However this turns out to be inconvenient as parts of the sheet assemble into thick bundles whereas the edge of the sheet does not lie in a single plane. Therefore we resort to a hot wire cutting tool to obtain cross-sections for one value of the control parameter Z_m (given in Table. I). With great care, one obtains neat cuts without perturbing the configuration. The cross-section is digitised with a scanner at a resolution of 50 pixels per mm, which yields 5 pixels for the thickness of the thinner sheets. A thresholding results in a binary image, from which empty spaces of surface area larger than $(10h)^2$ are kept, which removes light noise from the raw image (Fig. 1**b**. The binary image is skeletonized (reduced to a one pixel thick skeleton); junction points are then defined as pixels with at least 3 neighbours. Two neighbouring junction points delimit a stack of branches in close contact. The next step is to determine the number of branches in each of the M stacks. The conservation of the number of layers at each junction point yields $2M/3$ equations; the remaining $M/3$ equations are found from the thickness of the stacks in the binary image as follows. The heating by the cutting tool thickens (about twice) a stack nonlinearly, which was calibrated by separately cutting stacks of sheets. We keep the $M/3$ stacks with the best estimation of the thickness as given by the calibration. The solution of the linear $M \times M$ system yields the number of branches in each stack. We reopened a few configurations (5 per set of experiments) and checked by counting the number of branches in each stack; we found no error for sets ii and iii, and an error of ± 1 for a part of the thicker stacks (20%) in the more compact set i; these errors are small thanks to the fact that the number of layers is an integer. Thus, we obtain both the geometry and the topology of the sheet (Fig.1c,d). When repeating the experiment with the same experimental parameters, a whole variety of shapes is generated, which calls for a statistical approach. We systematically performed and analysed three sets of experiments (Table. I).

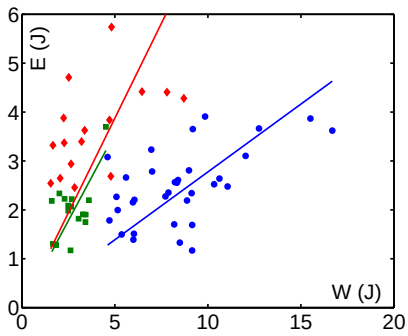

FIG. 2: Total elastic energy E (measured from the geometry) and injected work W for the three sets of experiments: i (circles), ii (squares) and iii (diamonds). The straight lines are fits to each set.

We first consider the global energetic quantities, injected work W and elastic energy E. Assuming the shape of the sheet to be exactly self-similar, a cross-section prescribes the energy of the whole sheet. Using (ρ, θ) the polar coordinates on the initially plane sheet, the branches, located in the plane $\rho \simeq Z_m$, have a local curvature $\kappa(\theta)$, and correspond to an angular sector on the sheet, where the curvature is $c(\rho, \theta) = Z_m\kappa(\theta)/\rho$, assuming the hole to be small $R \ll Z_m$. The bending energy E is

$$\frac{B}{2}\int_{R_c}^{r}\int_0^{2\pi} c^2\,\rho\text{d}\theta\,\text{d}\rho = \frac{BZ_m}{2}\,\ln\left(\frac{r}{R_c}\right)\int_0^{2\pi Z_m}\kappa^2(t)\,\text{d}t \quad (1)$$

where we introduced $t = Z_m\theta$, the curvilinear coordinate in the hole cross-section. The logarithmic prefactor known for d-cones [34] contains as cutoffs the radii of the mount R_c, and of the sheet r. In actual experiments, the self-similarity is not exact as some generators end below the mount; however this only slightly affects the logarithmic prefactor through the effective value of R_c. In order to account for plastic softening of the sheets, the quadratic κ^2 dependence of the energy was replaced by a linear dependance $\kappa_c(2\kappa - \kappa_c)$ for curvatures greater than the plastic threshold κ_c, measured as in [18] ($\kappa_c = 0.54\ mm^{-1}$, 0.24 mm^{-1} for $h = 0.05$ mm, 0.125 mm respectively). Fig. 2 shows the correlation between the bending energy E and the injected work W. It can be seen that the global quantities E and W fluctuate over the realisations as the system explores its configurational space. Energy dissipation occurs by friction between layers or with the container, and through discontinuous reorganisations when increasing the confinement (see [16]). The fluctuations in E and W can be ascribed to the differences in reorganisations according to realisations. E is roughly proportional

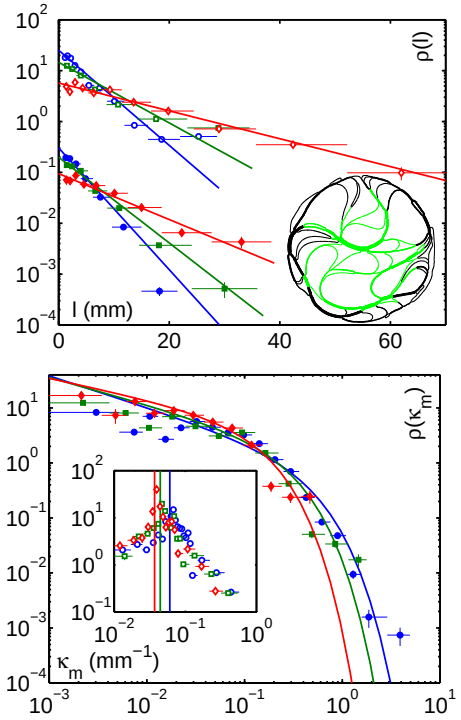

FIG. 3: The statistics of the geometrical properties for the three sets of experiments. **a** Length ℓ of branches and exponential distributions (Eq. 2). Circles for set i, squares for ii and diamonds for iii, empty for the periphery and full for the bulk. For the periphery $\rho(\ell)$ is multiplied by 10^2 for clarity. Means $\langle\ell\rangle = 3.3$, 4.5 mm for set i; 4.6, 6.8 mm for set ii; and 9.6, 16 mm for set iii, for the bulk and the periphery, respectively. The inset shows branches in the bulk (green) and at the periphery (dark). **c** Mean curvature of branches κ_m (same symbols as in **b**. For the bulk (main panel), the Gamma distribution (Eq. 3) with the same mean and variance is plotted; its exponent is $\alpha = 0.43$, 0.51 and 0.62 and its mean is $\langle\kappa_m\rangle = 0.16$, 0.12 and 0.08 mm^{-1}, for sets i, ii and iii, respectively. For the periphery (inset), the distribution are peaked at the curvature of the containers (shown by vertical lines).

to W, with a prefactor $a \lesssim 1$, suggesting that our geometrical estimation of the energy is consistent. ($a < 1$ because of dissipation.)

In the following we detail the main statistical properties measured over all realisations of a given set. Branches are good candidates to be elementary *particles* of the system, as elastic equilibrium imposes their shape given the boundary conditions, whereas the interaction between neighbouring branches is mediated by their extremities where contact forces and friction come into play.

For reasons which will become clear below, we split the system into two sub-systems (inset in Fig. 3**b**): branches with/without an extremity in contact with the container, which we will refer to as *periphery* and *bulk*, respectively. The lengths ℓ of branches follow exponential distributions (Fig. 3**b**)

$$f_{\rm E}(\ell) = 1/\mu \ \exp\left(-\ell/\mu\right). \qquad (2)$$

It appears that the value of the mean length $\langle\ell\rangle = \mu$ is larger for branches at the periphery than in the bulk, for each set of experiments. Next, we consider the absolute value of the average curvature $\kappa_{\rm m}$ of each branch (Fig. 3**c**). For the bulk, its distribution is well described by a Gamma law with density

$$f_{\rm G}^{\alpha,\chi}(\kappa_{\rm m}) = \frac{(\kappa_{\rm m}/\chi)^\alpha}{\Gamma(\alpha)\,\kappa_{\rm m}} \exp\left(-\frac{\kappa_{\rm m}}{\chi}\right), \qquad (3)$$

where Γ stands for Euler's Gamma function. In contrast, for the periphery, it is peaked at the value $1/R$ imposed by the container. Thus, the geometrical properties of the periphery and the bulk are significantly different.

set	$\langle e\rangle$ (mJ)	χ_e (mJ)	β^{-1} (mJ)	$\langle N_{br}\rangle$	$\langle E\rangle$ (J)
i	6.5	39	31	490	2.5
ii	6.6	35	28	360	2.0
iii	37	90	86	110	3.6

TABLE II: Temperatures: $\langle e\rangle$ is the mean energy per elementary *particle*, i.e. per branch; χ_e and β^{-1} are given by the tail of the distributions of energy in Fig. 4. Global quantities: total number of branches $\langle N_{br}\rangle$ and total energy $\langle E\rangle$ averaged over all realizations.

However, the distribution of the energy of the branches is the same for the two sub-systems as seen in Fig. 4. The energy e of a branch corresponds to that of an angular sector on the sheet and is calculated using equation 1, with limits of integration $t \in (0, \ell)$. The distributions of energy e are characterized by a power-law divergence at small values and by exponential tails (Fig. 4). They can be well described by Gamma laws $f_{\rm G}^{\alpha_e,\chi_e}(e)$ (Eq. 3) with intriguing values $\alpha_e < 1$, not trivialy interpretable as a number of subsystems as usually the case for values greater than 1 (see [19]). As many branches may be in the same state (when in the same stack), we also compared the distributions of energy to Bose-Einstein statistics

$$f_{\rm BE}(e) = \frac{A}{\exp\left(\beta e\right) - 1}, \qquad (4)$$

with zero chemical potential (the number of *particles* is unprescribed). The distributions of energy allow to define effective temperatures for each set of experiments: the mean energy per branch $\langle e\rangle$; and the characteristic energy given by the exponential tails $\chi_e \simeq \beta^{-1}$. The effective temperatures are ordered as $\langle e\rangle < \chi_e$ for each set of experiments (Table II); the sets of temperatures are close for the two sets of experiments with the same thickness h. Note that the ambient temperature $k_{\rm B}T = 4\ 10^{-21}$ J is negligible with respect to all temperatures defined here.

The identity of the distributions of energy between the bulk and the periphery, even though the geometrical properties differ, is our central result. Energy has contributions from both length and curvature. These two geometrical variables compensate so that the energy is statistically uniform. This means that *thermal equilibration* occurs between the two sub-systems. This equilibration justifies a description of the system in terms of statistical physics. Besides, our system is obviously not ergodic, as

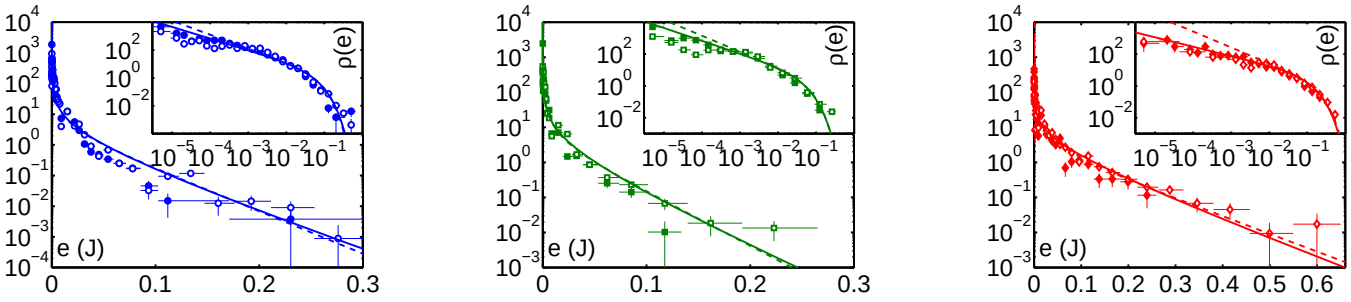

FIG. 4: Probability density functions of the energy e of the branches (elementary *particles*) for the three sets of experiments: *i* (**a**), *ii* (**b**) and *iii* (**c**). The distributions are given separately for the two sub-systems: bulk (full symbols) and periphery (open symbols); the fact that they are the same means that *thermal* equilibration occurs between the two sub-systems. The lines are Gamma distributions (continuous lines, Eq. 3) and Bose-Einstein distributions (dotted lines, Eq. 4) with the same mean and variance as the energy e. Gamma distributions have exponents $\alpha_e = 0.16$, 0.23 and 0.41, and Bose-Einstein distributions have prefactors $A = 4.0$, 5.1 and 3.0 J^{-1}, for sets *i*, *ii* and *iii*, respectively. The insets are log-log plots of the same data.

it must be driven by injecting work in order to explore the phase space. This driving has some similarities with the slow shearing of colloidal glasses [27] or granular materials [10, 29]; however, it is not stationary and restricts the accessible phase space at each reconfiguration of the sheet. As in other glassy systems, two different time scales characterise the dynamics: a very slow one associated with the driving and a quick one corresponding to the reconfiguration to local mechanical equilibrium. Finally, further experimental and theoretical work is needed to explain our observations. How universal are the distributions of energy? What controls the effective temperatures measured here?

We are grateful to Guillaume Angot for his experimental help. This study was supported by the EU through the NEST MechPlant project. LPS is associated with the universities of Paris VI and VII.

[1] H. M. Jaeger, S. R. Nagel, and R. P. Behringer, Rev. Mod. Phys. **68**, 1259 (1996).
[2] J. Bouchaud, L. F. Cugliandolo, J. Kurchan, and M. Mézard, in *Spin glasses and random fields*, edited by A. P. Young (World Scientific, Singapore, 1998).
[3] P. G. Debenedetti and F. Stillinger, Nature **410**, 259 (2001).
[4] S. F. Edwards and R. B. S. Oakeshott, Physica A pp. 1080–1090 (1989).
[5] L. F. Cugliandolo, J. Kurchan, and L. Peliti, Phys. Rev. E **55**, 3898 (1997).
[6] E. Bertin, O. Dauchot, and M. Droz, Phys. Rev. Lett. **96**, 120601 (2006).
[7] T. S. Grigera and N. E. Israeloff, Phys. Rev. Lett. **83**, 5038 (1999).
[8] L. Cugliandolo, D. R. Grempel, J. Kurchan, and E. Vincent, Europhys. Lett. **48**, 699 (1999).
[9] L. Bellon, S. Ciliberto, and C. Laroche, Europhys. Lett. **53**, 511 (2001).
[10] C. Song, O. Wang, and H. A. Makse, Proc. Nat. Acad. Sci. **102**, 2299 (2005).
[11] P. Wang, C. Song, and H. A. Makse, Nature Phys. **2**, 526 (2006).
[12] S. Jabbari-Farouji, D. Mizuno, M. Atakhorrami, F. C. MacKintosh, C. F. Schmidt, E. Eiser, G. H. Wegdam, and D. Bonn, Phys. Rev. Lett. **98**, 108302 (2007).
[13] L. Boué, M. Adda-Bedia, A. Boudaoud, D. Cassani, Y. Couder, A. Eddi, and M. Trejo, Phy. Rev. Lett. **97**, 166104 (2006).
[14] C. C. Donato, M. A. F. Gomes, and R. E. de Souza, Phys. Rev. E **67**, 026110 (2003).
[15] E. Katzav, M. Adda-Bedia, and A. Boudaoud, Proc. Nat. Acad. Sci. USA **103**, 18900 (2006).
[16] L. Boué and E. Katzav, EPL **80**, 54002 (2007).
[17] K. Matan, R. B. Williams, T. A. Witten, and S. R. Nagel, Phys. Rev. Lett. **88**, 076101 (2002).
[18] D. L. Blair and A. Kudrolli, Phys. Rev. Lett. **94**, 166107 (2005).
[19] E. Sultan and A. Boudaoud, Phys. Rev. Lett. **96**, 136103 (2006).
[20] A. S. Balankin, O. S. Huerta, R. C. M. de Oca, D. S. Ochoa, J. M. Trinidad, and M. A. Mendoza, Phys. Rev. E **74**, 061602 (2006).
[21] H. Kobayashi, B. Kresling, and J. F. V. Vincent, Proc. R. Soc. Lond. B **265**, 147 (1998).
[22] N. Kleckner, D. Zickler, G. H. Jones, J. Dekker, R. Padmore, J. Henle, and J. Hutchinson, Proc. Nat. Acad. Sci. USA **101**, 12592 (2004).
[23] P. K. Purohit, M. M. Inamdar, P. D. Grayson, T. M. Squires, J. Kondev, and R. Phillips, Biophys. J. **88**, 851 (2005).
[24] M. Schröter, D. I. Goldman, and H. L. Swinney, Phys. Rev. E **71**, 030301 (2005).
[25] F. Lechenault, F. da Cruz, O. Dauchot, and E. Bertin, J. Stat. Mech.: Theor. Exp. p. P07009 (2006).
[26] T. Aste, T. D. Matteo, M. Saadatfar, T. J. Senden, M. Schröter, and H. L. Swinney, EPL **79**, 24003 (2007).
[27] L. Berthier and A. Barrat, J. Chem. Phys. **116**, 6228 (2002).
[28] A. Barrat, J. Kurchan, V. Loreto, and M. Sellitto, Phys. Rev. Lett. **85**, 5034 (2000).
[29] H. A. Makse and J. Kurchan, Nature **415**, 614 (2002).
[30] I. K. Ono, C. S. O'Hern, D. J. Durian, S. A. Langer, A. J. Liu, and S. R. Nagel, Phys. Rev. Lett. **89**, 095703 (2002).
[31] D. S. Dean and A. Lefèvre, Phys. Rev. Lett. **90**, 198301 (2003).
[32] Y. Shokef and D. Levine, Phys. Rev. E **74**, 051111 (2006).
[33] S. Chaïeb, F. Melo, and J.-C. Géminard, Phys. Rev. Lett. **80**, 2354 (1998).

[34] M. Ben Amar and Y. Pomeau, Proc. R. Soc. Lond. A **453**, 729 (1997).